Science

Clonal hematopoiesis associated with TET2 deficiency accelerates atherosclerosis development in mice

José J. Fuster, Susan MacLauchlan, María A. Zuriaga, Maya N. Polackal, Allison C. Ostriker, Raja Chakraborty, Chia-Ling Wu, Soichi Sano, Sujatha Muralidharan, Cristina Rius, Jacqueline Vuong, Sophia Jacob, Varsha Muralidhar, Avril A. B. Robertson, Matthew A. Cooper, Vicente Andrés, Karen K. Hirschi, Kathleen A. Martin and Kenneth Walsh

Faulty blood cells and heart disease

Recent studies have shown that elderly people's blood cells often harbor mutations in genes encoding certain epigenetic regulators. These mutations can lead to clonal expansion of the mutant blood cells, which increases the risk of blood cancers and cardiovascular disease. Fuster *et al.* generated a mouse model to investigate how one of these genes, *Tet2*, affects atherosclerosis development (see the Perspective by Zhu *et al.*). They found that the disease progressed more rapidly in mice transplanted with *Tet2*-deficient bone marrow cells. This was due to increased secretion of interleukin-1 β by *Tet2*-deficient macrophages in a process that depended on the action of inflammasomes.

Science, this issue p. 842; see also p. 798

ARTICLE TOOLS	http://science.sciencemag.org/content/355/6327/842
SUPPLEMENTARY MATERIALS	http://science.sciencemag.org/content/suppl/2017/01/18/science.aag1381.DC1
RELATED CONTENT	http://science.sciencemag.org/content/sci/355/6327/798.full http://stke.sciencemag.org/content/sigtrans/10/464/eaah4214.full http://stke.sciencemag.org/content/sigtrans/9/419/ra29.full http://stm.sciencemag.org/content/scitransmed/8/333/333ra50.full http://stm.sciencemag.org/content/scitransmed/6/239/239sr1.full http://stm.sciencemag.org/content/scitransmed/7/275/275ra20.full http://stm.sciencemag.org/content/scitransmed/8/323/323ra13.full
REFERENCES	This article cites 30 articles, 9 of which you can access for free http://science.sciencemag.org/content/355/6327/842#BIBL
PERMISSIONS	http://www.sciencemag.org/help/reprints-and-permissions

REPORT

VASCULAR DISEASE

Clonal hematopoiesis associated with TET2 deficiency accelerates atherosclerosis development in mice

José J. Fuster,[1]* Susan MacLauchlan,[1] María A. Zuriaga,[1] Maya N. Polackal,[1] Allison C. Ostriker,[2] Raja Chakraborty,[2] Chia-Ling Wu,[1] Soichi Sano,[1] Sujatha Muralidharan,[1] Cristina Rius,[3] Jacquelyn Vuong,[1] Sophia Jacob,[1] Varsha Muralidhar,[1] Avril A. B. Robertson,[4] Matthew A. Cooper,[4] Vicente Andrés,[3] Karen K. Hirschi,[5] Kathleen A. Martin,[2] Kenneth Walsh[1]*

Human aging is associated with an increased frequency of somatic mutations in hematopoietic cells. Several of these recurrent mutations, including those in the gene encoding the epigenetic modifier enzyme TET2, promote expansion of the mutant blood cells. This clonal hematopoiesis correlates with an increased risk of atherosclerotic cardiovascular disease. We studied the effects of the expansion of Tet2-mutant cells in atherosclerosis-prone, low-density lipoprotein receptor–deficient ($Ldlr^{-/-}$) mice. We found that partial bone marrow reconstitution with TET2-deficient cells was sufficient for their clonal expansion and led to a marked increase in atherosclerotic plaque size. TET2-deficient macrophages exhibited an increase in NLRP3 inflammasome–mediated interleukin-1β secretion. An NLRP3 inhibitor showed greater atheroprotective activity in chimeric mice reconstituted with TET2-deficient cells than in nonchimeric mice. These results support the hypothesis that somatic TET2 mutations in blood cells play a causal role in atherosclerosis.

C ardiovascular disease (CVD) is the leading cause of death in the elderly, but almost 60% of elderly patients with atherosclerotic CVD have either no conventional risk factors (e.g., hypertension, hypercholesterolemia, etc.) or just one risk factor (1). Furthermore, increasing evidence suggests that most middle-aged individuals at low risk of CVD, based on conventional risk factors, exhibit subclinical atherosclerosis (2, 3). These clinical data suggest that unidentified age-dependent risk factors contribute to the development of CVD.

The accumulation of somatic DNA mutations is a hallmark of aging, particularly in proliferating tissues, which over time may become a mosaic of cells with different genotypes due to the clonal expansion of single de novo mutations (4). However, though human studies suggest that somatic mutations may be associated with a broad spectrum of human disease (5–7), there is little information on the potential causal role of somatic mutations in age-associated disorders other than cancer. Recent human studies have shown that normal aging is associated with an increased frequency of somatic mutations in the hematopoietic system, which provide a competitive growth advantage to the mutant cell and allow its progressive clonal expansion (clonal hematopoiesis) (7–11). This acquired clonal mosaicism in the hematopoietic system of healthy individuals correlates with an increased risk of subsequent hematologic cancer (7–9), but it has also been associated with higher prevalence of vascular complications of diabetes, greater incidence of atherosclerotic conditions (i.e., coronary heart disease, stroke), and increased frequency of CVD-related deaths (6, 7). Although these human studies suggest an unexpected connection between somatic mutations in hematopoietic cells, clonal hematopoiesis, and atherosclerosis, their descriptive nature does not allow cause-effect relationships, or even directionality, to be established.

Most of the reported somatic mutations associated with age-related clonal hematopoiesis occur in a small number of genes encoding epigenetic regulators (7–10). The present study focuses on one of these genes, TET2 (ten-eleven translocation 2), the first gene reported to exhibit somatic mutations in blood cells in individuals with clonal hematopoiesis without hematological malignancies (10). More than 70 different mutations have been reported in this gene (7–10, 12). The protein encoded by TET2 is an epigenetic regulatory enzyme that catalyzes the oxidation of 5-methylcytosine (5mc) in DNA to 5-hydroxymethylcytosine (5hmc) and also exerts noncatalytic actions. TET2 modulates hematopoietic stem and progenitor cell (HSPC) self-renewal (13–16), but its role in CVD remains largely unexplored.

To mimic the human scenario of clonal hematopoiesis and test whether clonal expansion of TET2-deficient hematopoietic cells contributes to atherosclerosis, we used a competitive bone marrow transplantation (BMT) strategy to generate atherosclerosis-prone, low-density lipoprotein receptor–deficient ($Ldlr^{-/-}$) chimeric mice with a small proportion of TET2-deficient HSPCs. Lethally irradiated $Ldlr^{-/-}$ recipients were transplanted with suspensions of bone marrow (BM) cells containing 10% $Tet2^{-/-}$ cells and 90% $Tet2^{+/+}$ cells [10% knockout (KO)–BMT mice] and then fed a normal diet (ND) or a high-fat/high-cholesterol (HFHC) diet for 9 weeks to induce atherosclerosis development (fig. S1). To distinguish donor $Tet2^{-/-}$ and $Tet2^{+/+}$ cells in this experimental setting, $Tet2^{+/+}$ cells were obtained from mice carrying the CD45.1 variant of the CD45 hematopoietic antigen, whereas $Tet2^{-/-}$ cells were obtained from mice carrying the CD45.2 variant of this protein. Control mice [10% wild-type (WT)–BMT] were transplanted with 10% CD45.2$^+$ $Tet2^{+/+}$ cells and 90% CD45.1$^+$ $Tet2^{+/+}$ cells. Flow cytometry analysis of CD45.2$^+$ blood cells established that this BMT strategy led to the clonal expansion of $Tet2^{-/-}$ hematopoietic cells to an extent consistent with variant allelic fractions for somatic TET2 mutations observed in human studies linking clonal hematopoiesis to accelerated CVD (7). At the start of ND or HFHC diet feeding (4 weeks after BMT), CD45.2$^+$ cells represented ~28% of blood cells in 10% KO-BMT mice, and they expanded further over time, reaching 42% of blood cells 6 weeks after BMT and 56% 12 weeks after BMT (Fig. 1, A and B). This clonal expansion of TET2-deficient hematopoietic cells is similar to that observed when human cells carrying somatic TET2 mutations are transplanted into immune-deficient mice (17).

TET2 ablation in CD45.2$^+$ cells of HFHC-fed 10% KO-BMT mice was confirmed by quantitative real-time polymerase chain reaction (qRT-PCR) analysis of CD45.2$^+$ white blood cell (WBC) fractions (Fig. 1C and fig. S2A). No changes were observed in the expression of TET1 or TET3, two related epigenetic modulators. Consistent with the enzymatic activity of TET2, ablation of the gene was paralleled by a decrease in 5hmC levels in WBCs and macrophages (fig. S2, B and C). Although the absolute number of HSPCs [defined as lineage$^-$, Sca1$^+$, c-Kit$^+$ (LSK) cells] was comparable between genotypes (fig. S3A), CD45.2$^+$ cells represented 69% of LSK cells in the BM (fig. S3B) and 61% in the spleen (fig. S3C) of 10% KO-BMT mice at 13 weeks post-BMT, consistent with previous studies reporting that TET2 inactivation enhances HSPC self-renewal (13–16).
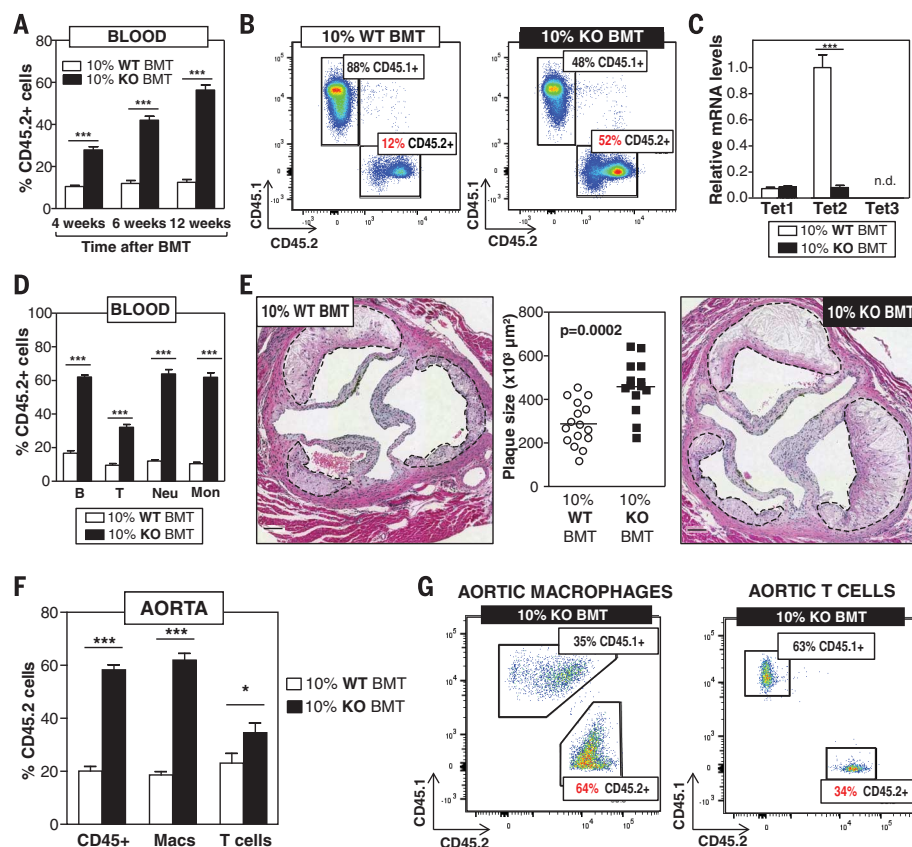
Fig. 1. Clonal expansion of TET2-deficient cells accelerates atherosclerosis in *Ldlr*$^{-/-}$ mice. 10% KO-BMT mice and 10% WT-BMT controls were fed a high-fat/high-cholesterol (HFHC) diet for 9 weeks, starting 4 weeks after BMT. (**A**) Percentage of CD45.2$^+$ WBCs in blood, evaluated by flow cytometry (*n* = 9 mice per genotype). (**B**) Representative images of CD45.1/CD45.2 flow cytometry analysis of WBC populations. (**C**) qRT-PCR analysis of TET2 transcript levels in CD45.2$^+$ WBCs from 10% WT-BMT (*n* = 14 mice) and 10% KO-BMT mice (*n* = 15 mice). (**D**) Percentage of CD45.2$^+$ cells within main blood cell lineages 13 weeks after BMT, measured by flow cytometry (*n* = 11 10% WT-BMT mice per genotype; *n* = 14 10% KO-BMT mice per genotype). (**E**) Aortic root plaque size. Representative images of hematoxylin and eosin (H&E)−stained sections are shown; atherosclerotic plaques are delineated by dashed lines. Scale bars, 100 μm. (**F**) Percentage of CD45.2$^+$ cells within the CD45$^+$ immune cell population, F4/80$^+$ macrophages (Macs), and CD3$^+$ T cells in the aortic arch (*n* = 4 pools of two aortic arches per genotype). (**G**) Representative images of CD45.1/CD45.2 flow cytometry analysis of aortic macrophages and T cells. Statistical significance was evaluated by two-way analysis of variance (ANOVA) with Sidak multiple comparison tests (*P < 0.05, ***P < 0.001) [(A), (C), (D), and (F)] and by two-tailed unpaired Student's *t* test (E). n.d., not detected. Error bars indicate SEM.

Transplanted *Tet2*$^{-/-}$ BM cells expanded into all blood cell lineages, regardless of type of diet, although with a slight myeloid bias and a reduced expansion into the T-lymphoid lineage in the BM, spleen, and blood (Fig. 1D and fig. S3, D to F), in agreement with previous studies with TET2-deficient mice (*13–16*). The expansion of *Tet2*$^{-/-}$ HSPCs did not affect blood cell counts (fig. S3G), consistent with findings in cancer-free individuals carrying *TET2* mutations in blood cells (*7, 10*).

Having demonstrated that the competitive BMT strategy leads to the clonal expansion of TET2-deficient HSPCs and mimics the human scenario of clonal hematopoiesis associated with *TET2* mutations, we next evaluated whether the clonal expansion of TET2-deficient HSPCs

affects atherogenesis and related metabolic abnormalities. We observed no effects on body weight (fig. S4A), spleen weight (fig. S4B), blood glucose levels (fig. S4C), systemic insulin sensitivity (fig. S4D), or plasma cholesterol levels (fig. S4E). ND-fed mice developed no aortic atherosclerosis, regardless of BM genotype (fig. S4F). In contrast, clonal expansion of TET2-deficient BM cells had a profound effect on HFHC-induced atherosclerosis, as 10% KO-BMT mice exhibited 60% larger plaques in the aortic root than did WT controls (Fig. 1E). Competitive BMT experiments with *Tet2*$^{+/-}$ cells revealed that TET2 heterozygosity is sufficient to accelerate atherosclerosis, despite the slower kinetics of TET2-heterozygous cell expansion (fig. S5). Increased atherogenesis in 10% KO-BMT mice was paral-

leled by an increase in total macrophage content in the intima, although this parameter was not statistically significant when normalized to plaque size (fig. S6). BM genotype did not affect lesional content of collagen or vascular smooth muscle cells (fig. S6), apoptosis (fig. S7A), necrotic core extension (fig. S7B), or proliferation rates of total plaque cells or lesional macrophages (fig. S7C). Overall, these data demonstrate that clonal expansion of TET2-deficient hematopoietic cells accelerates atherogenesis in a manner independent of alterations in systemic metabolism, changes in blood cell counts, or macrophage proliferation or apoptosis in the plaque.

Consistent with their above-mentioned preferential differentiation into myeloid cells, TET2-deficient HSPCs expanded preferentially into the macrophage population in the atherosclerotic vascular wall. CD45.2$^+$ cells represented 58% of total immune cells, 62% of macrophages, and 35% of T cells present in the aortic wall of 10% KO-BMT mice (Fig. 1, F and G, and fig. S8). On the basis of these findings, we hypothesized that TET2-deficient hematopoietic cells accelerate atherosclerosis mainly by generating a pool of macrophages with enhanced proatherogenic activities. To test this possibility, we used BMT and LysM-Cre/LoxP strategies to generate atherosclerosis-prone mice exhibiting TET2 deficiency restricted to myeloid cells (Mye-*Tet2*-KO mice). Although this strategy led to a partial (~80%) inactivation of *Tet2* in BM-derived macrophages (Fig. 2A), it was sufficient to increase plaque size in the aortic root of HFHC-fed mice (Fig. 2B), with no differences in body or spleen weight, blood monocyte counts, or glucose and cholesterol levels (fig. S9). These results demonstrate that TET2 deficiency in myeloid cells is sufficient to promote atherogenesis and suggest that macrophages play a major role in the accelerated atherosclerosis associated with expansion of TET2-deficient HSPCs. However, they do not rule out a potential contribution from other BM-derived cells. Analysis of aorta and aorta-draining mediastinal lymph nodes showed that the expansion of TET2-deficient HSPCs does not affect T cell numbers or aortic expression of T cell activation markers (fig. S10, A to C), although it leads to modest changes in the frequency of various T cell subsets (fig. S10, D to G), consistent with recent studies (*18, 19*). Such changes were not observed in Mye-*Tet2*-KO mice (fig. S10, H to J). Therefore, although a contribution of TET2-deficient T cells to the atherogenic effects of the expansion of TET2-deficient HSPCs cannot be excluded, these data demonstrate that changes in T cells are not essential for the accelerated atherosclerosis associated with TET2 loss of function and suggest instead a predominant role of macrophages in this context.

We next evaluated the effects of TET2 deficiency on the function of macrophages in culture. Consistent with the in vivo observations, TET2 deficiency did not affect macrophage proliferation (fig. S11A), apoptosis (fig. S11B),

oxidized low-density lipoprotein (oxLDL) uptake (fig. S11C), or the expression of cholesterol trafficking regulators (fig. S11, D and E). To evaluate whether TET2 deficiency affects proinflammatory macrophage activation, we performed Affymetrix microarray analysis on $Tet2^{-/-}$ macrophages and WT controls in resting conditions and after treatment with a combination of lipopolysaccharide (LPS) and interferon-γ (IFN-γ). Whereas no genes were differentially expressed in unstimulated macrophages (q value < 0.05; fig. S12), a widespread alteration in gene expression was found in $Tet2^{-/-}$ macrophages after a 10-hour treatment with LPS/IFN-γ. Expression of 475 genes was altered by more than a factor of 1.5 when compared with WT macrophages (q < 0.05; Fig. 2C). PANTHER functional annotation software revealed that transcripts encoding cytokine, chemokine, and signaling molecules were the top overrepresented classes altered in the transcriptome of LPS/IFN-γ–treated TET2-deficient macrophages (Fig. 2D). Genes in these classes with known proinflammatory actions were mostly up-regulated in TET2-deficient macrophages (Fig. 2E). Consistent with this observation, qRT-PCR analysis revealed that TET2-deficient macrophages exhibit markedly increased expression of proinflammatory cytokines (Fig. 2F and fig. S13, A and B), chemokines (fig. S13C), and enzymes (fig. S13D). This pattern of gene expression was also evident in $Tet2^{+/-}$ macrophages and macrophages isolated from Mye-$Tet2$-KO mice (fig. S13, E and F). TET2 deficiency also resulted in increased interleukin-6 (IL-6) protein levels in macrophage culture supernatants (fig. S13G). These data suggest that TET2 acts as a negative transcriptional regulator of proinflammatory responses and are consistent with a previous study reporting that TET2 represses LPS-induced IL-6 expression ([20]).

However, the situation in vivo in the atherosclerotic plaque is particularly complex, as lesional macrophages are exposed to multiple signals simultaneously. Therefore, the anti-inflammatory actions of TET2 in cultured macrophages were further evaluated by testing their effect on macrophage response to a cocktail of low doses of oxLDL, tumor necrosis factor (TNF), and IFN-γ, three stimuli present in atherosclerotic plaques. These conditions minimized the impact of TET2 deficiency on cytokine and chemokine expression (fig. S14), with the exception of IL-1β, which was markedly up-regulated in TET2-deficient macrophages at all time points of oxLDL/TNF/IFN-γ stimulation (Fig. 3A). Supporting a predominant role for IL-1β in the exacerbated atherosclerosis associated with TET2 loss of function, gene expression analysis of the aortic arch of HFHC-fed mice revealed a significant >twofold increase in transcript levels of IL-1β in 10% KO-BMT versus 10% WT-BMT mice (Fig. 3B), whereas few significant differences were observed in the aortic expression of other cytokines and chemokines or other macrophage-enriched genes (fig. S15). 10% KO-BMT also exhibited increased IL-1β protein levels in atherosclerotic plaques and plaque macrophages, as revealed by immunofluorescence staining coupled to confocal microscopy (Fig. 3, C and D).

To examine the molecular mechanisms underlying the effects of TET2 deficiency on IL-1β expression, we performed cell culture studies with LPS/IFN-γ–treated macrophages transiently overexpressing either WT TET2 or a TET2 mutant unable to catalyze the oxidation of 5mC to 5hmC. Both WT-TET2 and mutant-TET2 overexpression led to a ~90% reduction in IL-1β expression and blunted differences between $Tet2^{+/+}$ and $Tet2^{-/-}$ macrophages (Fig. 3E), suggesting that TET2 modulates IL-1β expression independent of its
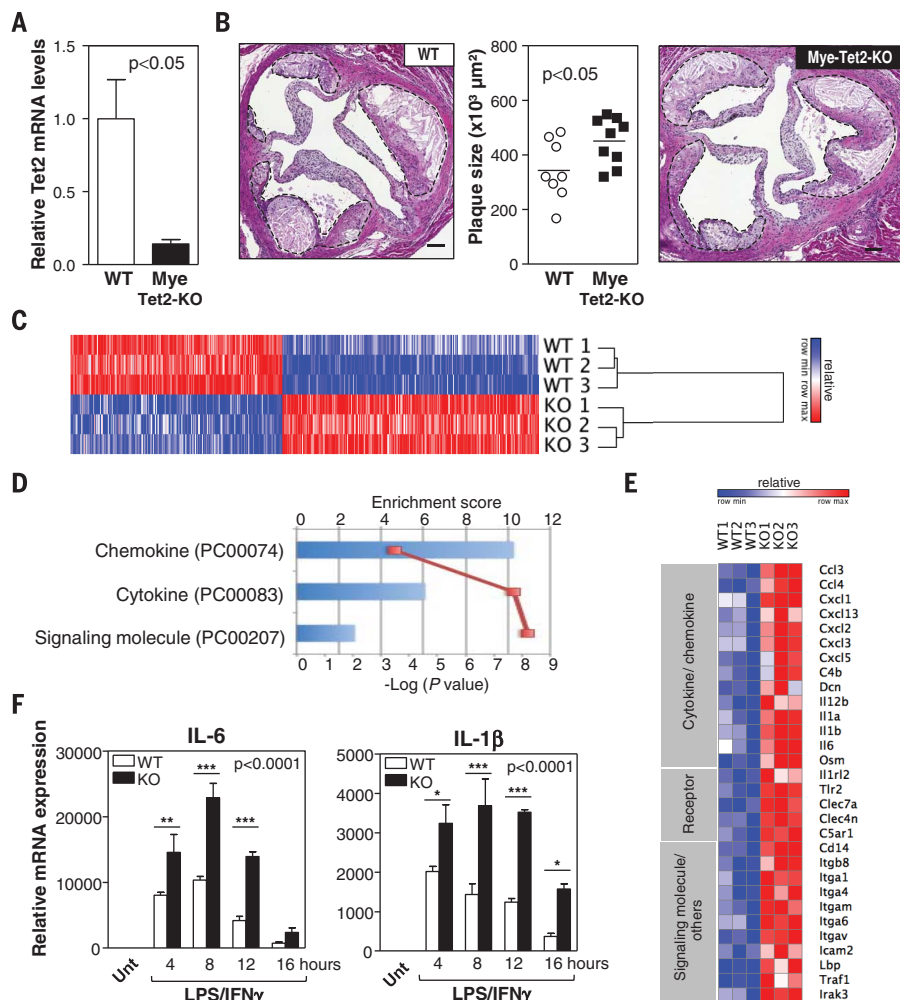

Fig. 2. TET2 deficiency in macrophages promotes inflammation and aggravates atherosclerosis.
(**A** and **B**) $Ldlr^{-/-}$ Mye-$Tet2$-KO mice (LysM-Cre$^+$ $Tet2^{flox/flox}$ BMT) and WT controls (LysM-Cre$^-$ $Tet2^{flox/flox}$ BMT) were fed a HFHC diet for 10 weeks. (A) qRT-PCR analysis of TET2 transcript levels in BM-derived macrophages isolated from Mye-$Tet2$-KO mice and WT controls (n = 6 mice per genotype). (B) Aortic root plaque size. Representative images of H&E-stained sections are shown; atherosclerotic plaques are delineated by dashed lines. Scale bars, 100 μm. (**C** to **F**) Peritoneal macrophages were isolated from $Tet2^{-/-}$ mice or WT controls [n = 3 mice per genotype in (C) to (E); n = 4 mice per genotype in (F)] and treated with 10 ng/ml LPS and 2 ng/ml IFN-γ to induce proinflammatory activation. (C) Heat map of genes with expression change exceeding a factor of 1.5 (q < 0.05) after 10 hours of LPS/IFN-γ stimulation, from a genome-wide expression profiling by microarray. (D) PANTHER analysis of genome-wide expression profiling by microarray. Three overrepresented classes were identified in $Tet2^{-/-}$ macrophages compared with all genes in Mus musculus (Bonferroni correction P < 0.05). (E) Heat map of selected genes up-regulated in $Tet2^{-/-}$ macrophages with expression change exceeding a factor of 1.5 (q < 0.05) from the genome-wide expression profiling by microarray. (F) qRT-PCR analysis of transcript levels of proinflammatory cytokines (IL-6 and IL-1β). Unt, untreated. Statistical significance was evaluated by two-tailed unpaired Student's t test with Welsh's correction (A), by two-tailed unpaired Student's t test (B), and by two-way ANOVA (P value for effect of genotype shown in graph) with Sidak multiple comparison tests (*P < 0.05, **P < 0.01, ***P < 0.001) (F). Error bars indicate SEM.

catalytic activity. Therefore, we investigated noncatalytic mechanisms of TET2-mediated transcriptional repression. Consistent with previous studies showing that TET2 inhibits gene transcription via histone deacetylase (HDAC)–mediated histone deacetylation (20), treatment with the HDAC inhibitor trichostatin A (TSA) increased IL-1β expression in LPS/IFN-γ–treated macrophages and abolished expression differences between TET2-deficient and WT genotypes (Fig. 3F). Further supporting a role for histone deacetylation in TET2-mediated repression of IL-1β, chromatin immunoprecipitation (ChIP)–qPCR analysis revealed greater histone H3 acetylation at the *Il1b* gene promoter in TET2-deficient macrophages (Fig. 3G). In contrast, treatment with TSA reduced the expression of transcripts corresponding to other proinflammatory cytokines (such as IL-6), in agreement with previous reports (21), and did not affect differences between genotypes (fig. S16A). Furthermore, H3 acetylation at the *Il6* gene promoter was not affected by TET2 ablation (fig. S16B). Overall, these data suggest that a reduction in HDAC-mediated histone deacetylation accounts for the effects of TET2 loss of function on IL-1β expression in macrophages, whereas alternative mechanisms contribute to its effects on other genes.

Given that IL-1β is synthesized as an inactive protein (pro–IL-1β), which requires cleavage for its secretion, the effects of TET2 deficiency on IL-1β posttranslational processing were also evaluated. IL-1β cleavage is frequently mediated by the NLRP3 inflammasome, a multiprotein complex that is activated by "danger signals" (intracellular molecules that are released as a result of disturbance of tissue homeostasis). NLRP3 inflammasome activation is typically a two-step process requiring a priming signal, which promotes pro–IL-1β/NLRP3 expression, and an activation signal, which promotes inflammasome assembly. To investigate whether TET2 deficiency facilitates NLRP3-mediated IL-1β processing, IL-1β cleavage was evaluated by Western blot in LPS/IFN-γ–primed macrophages treated with adenosine triphosphate (ATP) for inflammasome activation. TET2-deficient macrophages exhibited significant increases in intracellular pro–IL-1β and cleaved IL-1β (Fig. 4, A and B). However, the effect on cleaved IL-1β levels (2.5-fold; Fig. 4B) was substantially greater than that on pro–IL-1β levels (1.6-fold; Fig. 4A), which suggests that TET2 loss of function promotes IL-1β secretion by macrophages beyond its effects on IL-1β transcription. Consistent with these findings, Western blot (Fig. 4C) and enzyme-linked immunosorbent assay (ELISA) analysis (Fig. 4D) revealed a >threefold increase in secreted IL-1β levels in LPS/IFN-γ/ATP–treated TET2-deficient macrophages. IL-1β secretion was completely abrogated by cotreatment with MCC950 (Fig. 4D), a specific NLRP3 inhibitor (22), which suggests that TET2 deficiency affects NLRP3-mediated IL-1β secretion.

To further test this possibility, we evaluated the effect of TET2 on the expression of the main NLRP3 inflammasome components. TET2 deficiency significantly increased NLRP3 expression in LPS/IFN-γ–treated (fig. S17, A and B) and oxLDL/TNF/IFN-γ–treated macrophages (fig. S17C), whereas no change was observed in the expression of other inflammasome components (fig. S17, D and E). TET2 deficiency also enhanced IL-1β secretion induced by cotreatment with cholesterol crystals (Fig. 4E), a relevant inducer of inflammasome activation in atherosclerosis (23). Increased activity of caspase 1 (enzymatic component of the NLRP3 inflammasome) was detected in plaque macrophages of 10% KO-BMT mice, as revealed by FAM-YVAD-FMK fluorescent staining with a FLICA probe (Fig. 4F), supporting the hypothesis that TET2 ablation enhances NLRP3 inflammasome activity in vivo in the atherosclerotic plaque. Overall, these data demonstrate that TET2 deficiency contributes to IL-1β production in macrophages by enhancing NLRP3 priming in addition to promoting *Il1b* gene transcription. The data are also consistent with a central role of enhanced IL-1β signaling in the increased atherosclerosis associated with expansion of TET2-deficient hematopoietic cells. In support of this idea, when 10% KO-BMT mice were continuously infused with the NLRP3 inhibitor MCC950, the difference in aortic plaque size between these chimeric mice and the nonchimeric control mice was eliminated (Fig. 4G). This MCC950 treatment did not affect the expansion of TET2-deficient cells (fig. S18). These studies revealed that MCC950 exerts greater atheroprotective actions in conditions of clonal hematopoiesis associated with TET2 deficiency, as it decreased atherosclerotic plaque size by ~50% in 10% KO-BMT mice, whereas it led to a nonstatistically significant ~20% reduction in 10% WT-BMT controls. Overall, these studies demonstrate that NLRP3-mediated IL-1β overproduction is essential for the atherogenic consequences of clonal expansion of TET2-deficient cells.

Having demonstrated the role of NLRP3-mediated IL-1β secretion, we next explored potential atherogenic mechanisms downstream of this proinflammatory cytokine. The proatherogenic actions of IL-1 signaling are mediated primarily by its effects on vascular cells (24), and IL-1β modulates endothelial cell adhesion expression in various settings (24–26). On the basis of these findings and the key role of endothelial cell activation in early atherogenesis, we
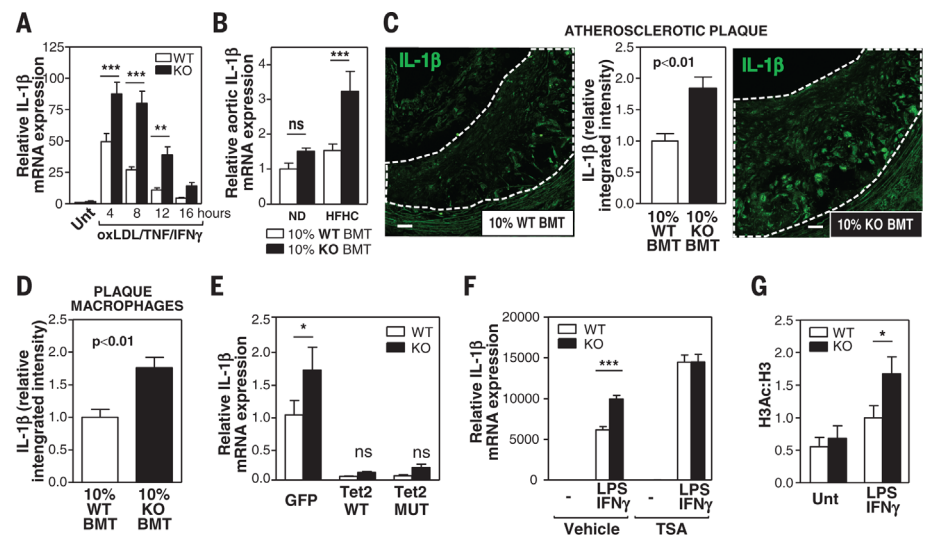

Fig. 3. TET2 regulates IL-1β expression in macrophages. (**A** and **B**) qRT-PCR analysis of IL-1β expression in *Tet2*−/− and *Tet2*+/+ peritoneal macrophages treated with 25 μg/ml oxidized LDL (oxLDL), 5 ng/ml TNF, and 2 ng/ml IFN-γ [(A), n = 6 mice per genotype] or in aortic arch samples (B) obtained from ND- or HFHC-fed 10% WT-BMT mice (n = 10 ND, 9 HFHC) and 10% KO-BMT mice (n = 8 ND, 8 HFHC). (**C** and **D**) IL-1β immunofluorescent staining in aortic root plaques (C) or CD68+ macrophage-rich areas (D) of 10% KO-BMT mice and 10% WT-BMT controls (n = 6 mice per genotype), quantified as integrated fluorescence intensity normalized to plaque or macrophage area. Representative images of IL-1β–stained plaques are shown. Dashed lines indicate plaques. Scale bars, 30 μm. (**E**) qRT-PCR analysis of IL-1β expression in *Tet2*−/− and *Tet2*+/+ peritoneal macrophages (n = 3 mice per genotype) transiently overexpressing WT TET2, catalytically inactive mutant TET2, or GFP as control. Macrophages were treated for 6 hours with 10 ng/ml LPS and 2 ng/ml IFN-γ. (**F**) qRT-PCR analysis of IL-1β expression in macrophages isolated from *Tet2*−/− or *Tet2*+/+ mice (n = 3 mice per genotype) and treated for 8 hours with LPS/IFN-γ in the absence or presence of 0.5 μM trichostatin A (TSA). (**G**) ChIP-qPCR analysis of H3 acetylation in the IL-1β promoter of macrophages isolated from *Tet2*−/− or *Tet2*+/+ mice (n = 6 to 8 mice per genotype and condition). Statistical significance was evaluated by two-way ANOVA with Sidak multiple comparison test [nonsignificant (ns) P > 0.4, *P < 0.05, **P < 0.01, ***P < 0.001] [(A), (B), and (E) to (G)] and by two-tailed unpaired Student's *t* test [(C) and (D)]. Error bars indicate SEM.
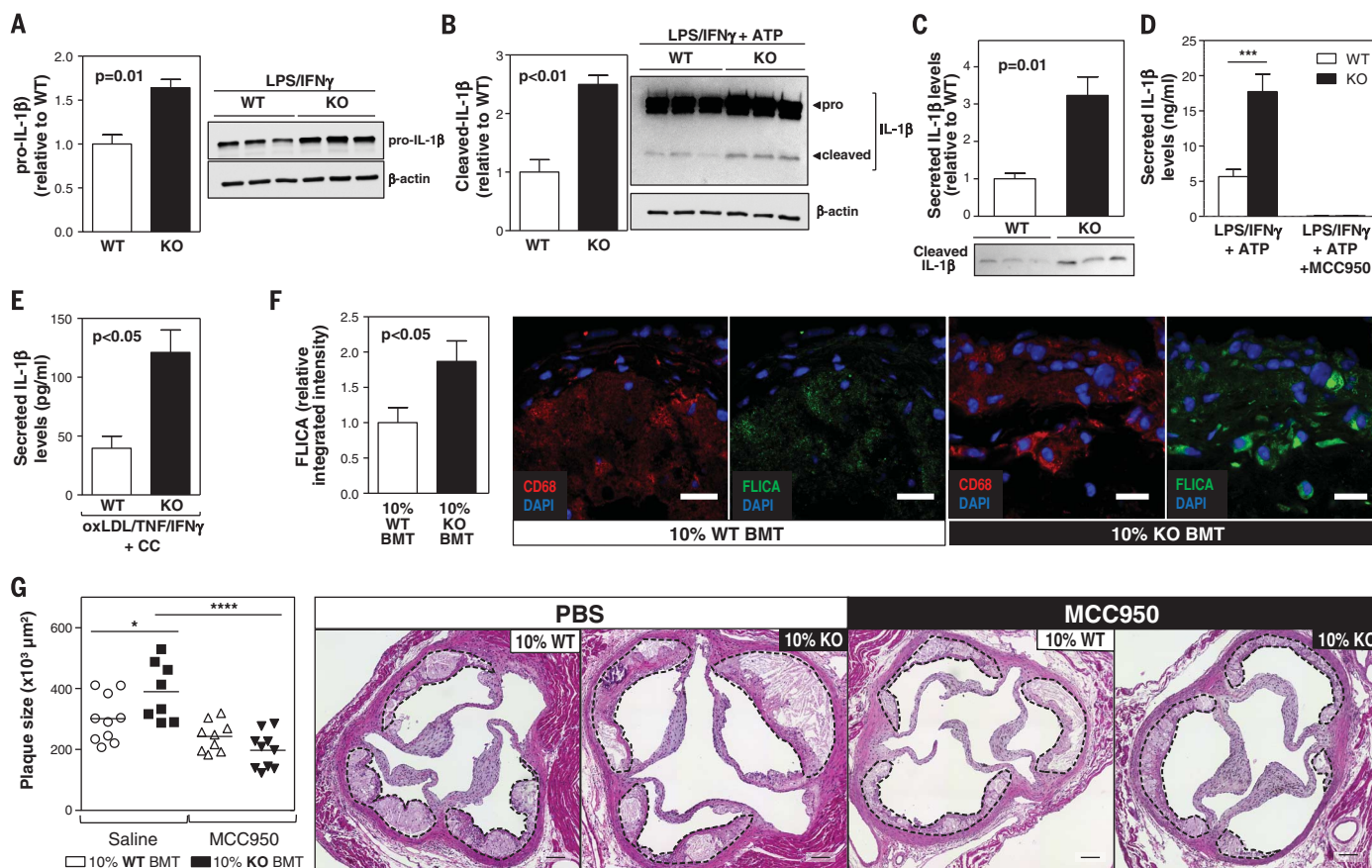
Fig. 4. The NLRP3 inflammasome is essential for the exacerbated atherosclerosis associated with clonal expansion of TET2-deficient hematopoietic cells. (**A** and **B**) Western blot analysis of intracellular IL-1β in peritoneal macrophages isolated from $Tet2^{-/-}$ mice and $Tet2^{+/+}$ controls ($n = 3$ mice per genotype) after 6 hours of treatment with 10 ng LPS and 2 ng IFN-γ (A) or after the same treatment combined with a final 15-min incubation with 5 mM ATP (B). Data were normalized to β-actin levels. (**C**) Western blot analysis of IL-1β in the supernatant of $Tet2^{-/-}$ and $Tet2^{+/+}$ macrophages ($n = 3$ mice per genotype) after 6 hours of LPS/IFN-γ treatment combined with a final 30-min incubation with ATP. (**D**) ELISA analysis of IL-1β in the supernatant of $Tet2^{-/-}$ and $Tet2^{+/+}$ macrophages ($n = 3$ mice per genotype) after 6 hours of LPS/IFN-γ treatment combined with a final 30-min incubation with 5 mM ATP in the presence or absence of 10 μM MCC950. (**E**) ELISA analysis of IL-1β in the supernatant of $Tet2^{-/-}$ and $Tet2^{+/+}$ macrophages ($n = 3$ mice per genotype) after 8 hours of oxLDL/TNF/IFN-γ

stimulation in the presence of 1 mg/ml cholesterol crystals (CC). (**F**) Caspase 1 activity detected by fluorescent staining with a FAM-YVAD-FMK FLICA reagent in CD68+ macrophage-rich areas of HFHC-fed 10% KO-BMT mice and 10% WT-BMT controls ($n = 6$ mice per genotype), quantified as integrated fluorescence intensity normalized to macrophage area. Representative images are shown. DAPI, 4′,6-diamidino-2-phenylindole. Scale bars, 25 μm. (**G**) Aortic root plaque size in HFHC-fed 10% KO-BMT and 10% WT-BMT mice. Mice received a continuous infusion of MCC950 (5 mg per kg per day) or phosphate-buffered saline vehicle via subcutaneous osmotic pumps. Representative images of H&E-stained sections are shown; plaques are delineated by dashed lines. Scale bars, 100 μm. Statistical significance was evaluated by two-tailed unpaired Student's t tests [(A) to (C), (E), and (F)], by two-way ANOVA with Sidak multiple comparison test (D), and by two-way ANOVA with Tukey multiple comparison test (G) (*$P < 0.05$, ***$P < 0.001$, ****$P < 0.001$). Error bars indicate SEM.

evaluated whether the increased IL-1β expression in 10% KO-BMT mice was paralleled by changes in the aortic expression of endothelial adhesion molecules. The expression of P-selectin was significantly increased in HFHC-fed 10% KO-BMT mice (fig. S19A), and there was a significant correlation between IL-1β and P-selectin expression in the aorta (fig. S19B). MCC950 treatment abrogated the increased expression of P-selectin in 10% KO-BMT mice (fig. S19C), supporting the contribution of IL-1β to the aortic expression of P-selectin. Given the major role of P-selectin in monocyte recruitment to the atherosclerotic plaque, we hypothesized that TET2-deficient macrophages contribute to endothelial cell activation and monocyte recruitment. Supporting this

hypothesis, leukocyte homing experiments based on the adoptive transfer of green fluorescent protein+ (GFP+) (Tet2-WT) myeloid cells revealed increased recruitment to the aortic wall of Mye-Tet2-KO mice compared with WT controls (fig. S19D).

In summary, our results support a causal link between exacerbated atherosclerosis and clonal hematopoiesis induced by somatic mutations. Combined with the observations made in human studies (7), our mouse data suggest that somatic TET2 mutations could potentially be targeted for the development of new therapies or preventive care strategies for atherosclerosis. Furthermore, when considered in light of previous cancer studies (12, 14, 15), these results support the

notion that the expansion of TET2-mutant HSPCs represents a pathophysiological mechanism that is shared between blood cancers and CVD. Our study also revealed that exacerbated NLRP3-mediated IL-1β production is essential for accelerated atherosclerosis in a context of clonal hematopoiesis due to TET2 loss of function. IL-1β is a potential therapeutic target in the setting of atherosclerosis, and neutralizing anti–IL-1β antibodies are being evaluated in clinical trials for the treatment of CVD (27). Our findings suggest that IL-1β blockade or NLRP3 inflammasome inhibition may be particularly effective for the prevention and treatment of CVD in individuals carrying somatic mutations in TET2. Future studies are warranted to address this possibility.

REFERENCES AND NOTES

1. U. N. Khot, M. B. Khot, C. T. Bajzer, S. K. Sapp, E. M. Ohman, S. J. Brener, S. G. Ellis, A. M. Lincoff, E. J. Topol, *JAMA* **290**, 898–904 (2003).
2. L. Fernández-Friera, J. L. Peñalvo, A. Fernández-Ortiz, B. Ibáñez, B. López-Melgar, M. Laclaustra, B. Oliva, A. Mocoroa, J. Mendiguren, V. Martínez de Vega, L. García, J. Molina, J. Sánchez-González, G. Guzmán, J. C. Alonso-Farto, E. Guallar, F. Civeira, H. Sillesen, S. Pocock, J. M. Ordovás, G. Sanz, L. J. Jiménez-Borreguero, V. Fuster, *Circulation* **131**, 2104–2113 (2015).
3. M. Laclaustra, J. A. Casasnovas, A. Fernández-Ortiz, V. Fuster, M. León-Latre, L. J. Jiménez-Borreguero, M. Pocovi, Y. Hurtado-Roca, J. M. Ordovas, E. Jarauta, E. Guallar, B. Ibáñez, F. Civeira, *J. Am. Coll. Cardiol.* **67**, 1263–1274 (2016).
4. J. Vijg, *Curr. Opin. Genet. Dev.* **26**, 141–149 (2014).
5. A. Poduri, G. D. Evrony, X. Cai, C. A. Walsh, *Science* **341**, 1237758 (2013).
6. A. Bonnefond, B. Skrobek, S. Lobbens, E. Eury, D. Thuillier, S. Cauchi, O. Lantieri, B. Balkau, E. Riboli, M. Marre, G. Charpentier, L. Yengo, P. Froguel, *Nat. Genet.* **45**, 1040–1043 (2013).
7. S. Jaiswal, P. Fontanillas, J. Flannick, A. Manning, P. V. Grauman, B. G. Mar, R. C. Lindsley, C. H. Mermel, N. Burtt, A. Chavez, J. M. Higgins, V. Moltchanov, F. C. Kuo, M. J. Kluk, B. Henderson, L. Kinnunen, H. A. Koistinen, C. Ladenvall, G. Getz, A. Correa, B. F. Banahan, S. Gabriel, S. Kathiresan, H. M. Stringham, M. I. McCarthy, M. Boehnke, J. Tuomilehto, C. Haiman, L. Groop, G. Atzmon, J. G. Wilson, D. Neuberg, D. Altshuler, B. L. Ebert, *N. Engl. J. Med.* **371**, 2488–2498 (2014).
8. M. Xie, C. Lu, J. Wang, M. D. McLellan, K. J. Johnson, M. C. Wendl, J. F. McMichael, H. K. Schmidt, V. Yellapantula, C. A. Miller, B. A. Ozenberger, J. S. Welch, D. C. Link, M. J. Walter, E. R. Mardis, J. F. Dipersio, F. Chen, R. K. Wilson, T. J. Ley, L. Ding, *Nat. Med.* **20**, 1472–1478 (2014).
9. G. Genovese, A. K. Kähler, R. E. Handsaker, J. Lindberg, S. A. Rose, S. F. Bakhoum, K. Chambert, E. Mick, B. M. Neale, M. Fromer, S. M. Purcell, O. Svantesson, M. Landén, M. Höglund, S. Lehmann, S. B. Gabriel, J. L. Moran, E. S. Lander, P. F. Sullivan, P. Sklar, H. Grönberg, C. M. Hultman, S. A. McCarroll, *N. Engl. J. Med.* **371**, 2477–2487 (2014).
10. L. Busque, J. P. Patel, M. E. Figueroa, A. Vasanthakumar, S. Provost, Z. Hamilou, L. Mollica, J. Li, A. Viale, A. Heguy, M. Hassimi, N. Socci, P. K. Bhatt, M. Gonen, C. E. Mason, A. Melnick, L. A. Godley, C. W. Brennan, O. Abdel-Wahab, R. L. Levine, *Nat. Genet.* **44**, 1179–1181 (2012).
11. T. McKerrell, N. Park, T. Moreno, C. S. Grove, H. Ponstingl, J. Stephens, C. Crawley, J. Craig, M. A. Scott, C. Hodkinson, J. Baxter, R. Rad, D. R. Forsyth, M. A. Quail, E. Zeggini, W. Ouwehand, I. Varela, G. S. Vassiliou; Understanding Society Scientific Group, *Cell Reports* **10**, 1239–1245 (2015).
12. M. Ko, Y. Huang, A. M. Jankowska, U. J. Pape, M. Tahiliani, H. S. Bandukwala, J. An, E. D. Lamperti, K. P. Koh, R. Ganetzky, X. S. Liu, L. Aravind, S. Agarwal, J. P. Maciejewski, A. Rao, *Nature* **468**, 839–843 (2010).
13. M. Ko, H. S. Bandukwala, J. An, E. D. Lamperti, E. C. Thompson, R. Hastie, A. Tsangaratou, K. Rajewsky, S. B. Koralov, A. Rao, *Proc. Natl. Acad. Sci. U.S.A.* **108**, 14566–14571 (2011).
14. K. Moran-Crusio, L. Reavie, A. Shih, O. Abdel-Wahab, D. Ndiaye-Lobry, C. Lobry, M. E. Figueroa, A. Vasanthakumar, J. Patel, X. Zhao, F. Perna, S. Pandey, J. Madzo, C. Song, Q. Dai, C. He, S. Ibrahim, M. Beran, J. Zavadil, S. D. Nimer, A. Melnick, L. A. Godley, I. Aifantis, R. L. Levine, *Cancer Cell* **20**, 11–24 (2011).
15. C. Quivoron, L. Couronné, V. Della Valle, C. K. Lopez, I. Plo, O. Wagner-Ballon, M. Do Cruzeiro, F. Delhommeau, B. Arnulf, M.-H. Stern, L. Godley, P. Opolon, H. Tilly, E. Solary, Y. Duffourd, P. Dessen, H. Merle-Beral, F. Nguyen-Khac, M. Fontenay, W. Vainchenker, C. Bastard, T. Mercher, O. A. Bernard, *Cancer Cell* **20**, 25–38 (2011).
16. Z. Li, X. Cai, C.-L. Cai, J. Wang, W. Zhang, B. E. Petersen, F.-C. Yang, M. Xu, *Blood* **118**, 4509–4518 (2011).
17. F. Delhommeau, S. Dupont, V. Della Valle, C. James, S. Trannoy, A. Massé, O. Kosmider, J.-P. Le Couedic, F. Robert, A. Alberdi, Y. Lécluse, I. Plo, F. J. Dreyfus, C. Marzac, N. Casadevall, C. Lacombe, S. P. Romana, P. Dessen, J. Soulier, F. Viguié, M. Fontenay, W. Vainchenker, O. A. Bernard, *N. Engl. J. Med.* **360**, 2289–2301 (2009).
18. R. Yang, C. Qu, Y. Zhou, J. E. Konkel, S. Shi, Y. Liu, C. Chen, S. Liu, D. Liu, Y. Chen, E. Zandi, W. Chen, Y. Zhou, S. Shi, *Immunity* **43**, 251–263 (2015).
19. X. Yue, S. Trifari, T. Äijö, A. Tsagaratou, W. A. Pastor, J. A. Zepeda-Martínez, C.-W. J. Lio, X. Li, Y. Huang, P. Vijayanand, H. Lähdesmäki, A. Rao, *J. Exp. Med.* **213**, 377–397 (2016).
20. Q. Zhang, K. Zhao, Q. Shen, Y. Han, Y. Gu, X. Li, D. Zhao, Y. Liu, C. Wang, X. Zhang, X. Su, J. Liu, W. Ge, R. L. Levine, N. Li, X. Cao, *Nature* **525**, 389–393 (2015).
21. T. Roger, J. Lugrin, D. Le Roy, G. Goy, M. Mombelli, T. Koessler, X. C. Ding, A.-L. Chanson, M. K. Reymond, I. Miconnet, J. Schrenzel, P. François, T. Calandra, *Blood* **117**, 1205–1217 (2011).
22. R. C. Coll, A. A. Robertson, J. J. Chae, S. C. Higgins, R. Muñoz-Planillo, M. C. Inserra, I. Vetter, L. S. Dungan, B. G. Monks, A. Stutz, D. E. Croker, M. S. Butler, M. Haneklaus, C. E. Sutton, G. Núñez, E. Latz, D. L. Kastner, K. H. Mills, S. L. Masters, K. Schroder, M. A. Cooper, L. A. O'Neill, *Nat. Med.* **21**, 248–255 (2015).
23. P. Duewell, H. Kono, K. J. Rayner, C. M. Sirois, G. Vladimer, F. G. Bauernfeind, G. S. Abela, L. Franchi, G. Nuñez, M. Schnurr, T. Espevik, E. Lien, K. A. Fitzgerald, K. L. Rock, K. J. Moore, S. D. Wright, V. Hornung, E. Latz, *Nature* **464**, 1357–1361 (2010).
24. S. Shemesh, Y. Kamari, A. Shaish, S. Olteanu, M. Kandel-Kfir, T. Almog, I. Grosskopf, R. N. Apte, D. Harats, *Atherosclerosis* **222**, 329–336 (2012).
25. T. Kirii, T. Niwa, Y. Yamada, H. Wada, K. Saito, Y. Iwakura, M. Asano, H. Moriwaki, M. Seishima, *Arterioscler. Thromb. Vasc. Biol.* **23**, 656–660 (2003).
26. H. B. Sager, T. Heidt, M. Hulsmans, P. Dutta, G. Courties, M. Sebas, G. R. Wojtkiewicz, B. Tricot, Y. Iwamoto, Y. Sun, R. Weissleder, P. Libby, F. K. Swirski, M. Nahrendorf, *Circulation* **132**, 1880–1890 (2015).
27. P. M. Ridker, T. F. Lüscher, *Eur. Heart J.* **35**, 1782–1791 (2014).

SUPPLEMENTARY MATERIALS

www.sciencemag.org/content/355/6327/842/suppl/DC1
Materials and Methods
Figs. S1 to S19
References (*28–30*)